J Appl Physiol 131: 746–759, 2021.
First published June 17, 2021; doi:10.1152/japplphysiol.00132.2021

american physiological society | JOURNAL OF APPLIED PHYSIOLOGY

RESEARCH ARTICLE

Selectivity and excitability of upper-limb muscle activation during cervical transcutaneous spinal cord stimulation in humans

Roberto M. de Freitas,[1] Atsushi Sasaki,[2,3] Dimitry G. Sayenko,[4] Yohei Masugi,[2,5] Taishin Nomura,[1] Kimitaka Nakazawa,[2] and Matija Milosevic[1]

[1]*Department of Mechanical Science and Bioengineering, Graduate School of Engineering Science, Osaka University, Toyonaka, Japan;* [2]*Department of Life Sciences, Graduate School of Arts and Sciences, The University of Tokyo, Meguro, Japan;* [3]*Japan Society for the Promotion of Science, Chiyoda, Japan;* [4]*Department of Neurosurgery, Center for Neuroregeneration, Houston Methodist Research Institute, Houston, Texas; and* [5]*Institute of Sports Medicine and Science, Tokyo International University, Kawagoe, Japan*

Abstract

Cervical transcutaneous spinal cord stimulation (tSCS) efficacy for rehabilitation of upper-limb motor function was suggested to depend on recruitment of Ia afferents. However, selectivity and excitability of motor activation with different electrode configurations remain unclear. In this study, activation of upper-limb motor pools was examined with different cathode and anode configurations during cervical tSCS in 10 able-bodied individuals. Muscle responses were measured from six upper-limb muscles simultaneously. First, postactivation depression was confirmed with tSCS paired pulses (50-ms interval) for each cathode configuration (C6, C7, and T1 vertebral levels), with anode on the anterior neck. Selectivity and excitability of activation of the upper-limb motor pools were examined by comparing the recruitment curves (10–100 mA) of first evoked responses across muscles and cathode configurations. Our results showed that hand muscles were preferentially activated when the cathode was placed over T1 compared with the other vertebral levels, whereas there was no selectivity for proximal arm muscles. Furthermore, higher stimulation intensities were required to activate distal hand muscles than proximal arm muscles, suggesting different excitability thresholds between muscles. In a separate protocol, responses were compared between anode configurations (anterior neck, shoulders, iliac crests, and back), with one selected cathode configuration. The level of discomfort was also assessed. Largest muscle responses were elicited with the anode configuration over the anterior neck, whereas there were no differences in the discomfort. Our results therefore inform methodological considerations for electrode configuration to help optimize recruitment of Ia afferents during cervical tSCS.

NEW & NOTEWORTHY We examined selectivity and excitability of motor activation in multiple upper-limb muscles during cervical transcutaneous spinal cord stimulation with different cathode and anode configurations. Hand muscles were more activated when the cathode was configured over the T1 vertebra compared with C6 and C7 locations. Higher stimulation intensities were required to activate distal hand muscles than proximal arm muscles. Finally, configuration of anode over anterior neck elicited larger responses compared with other configurations.

cervical; postactivation depression; reflex; transcutaneous spinal cord stimulation; upper-limbs

INTRODUCTION

Epidural stimulation of cervical spinal cord has been used to restore upper-limb movements after spinal cord injury (SCI) (1). Similarly, noninvasive cervical transcutaneous spinal cord stimulation (tSCS) has recently gained considerable interest in rehabilitation of upper-limb motor function after SCI (2–5). Although both approaches may activate common neural structures within the spinal cord (6), the extent of selectivity of activation of upper-limb muscles using different cathode and anode configurations with tSCS remains unclear.

Electrical impulses reaching the spinal cord using either surface or implanted electrodes can activate monosynaptic and oligosynaptic connections between sensory afferents and α-motoneurons (6–8). Such transsynaptic activation of muscles may compensate for the scarce, or even absent, proprioceptive information during motor tasks in individuals with SCI (4, 9, 10). Specifically, excitation of Ia monosynaptic pathways was suggested to be critical for strengthening descending commands through the spinal lesioned site to caudal levels and may promote reorganization of neural motor pathways (9, 11–13). Paired pulses delivered using tSCS with short interstimulus intervals (e.g., 50 ms) can be used to test

Correspondence: M. Milosevic (matija@bpe.es.osaka-u.ac.jp).
Submitted 26 February 2021 / Revised 19 May 2021 / Accepted 12 June 2021

the excitation of Ia monosynaptic pathways by confirming suppression of the second evoked response in relation to the first (14, 15). Although other sensory fibers and interneurons may also be excited, it was previously suggested that suppression may primarily be attributed to postactivation depression (16). Such mechanism can be used to confirm the reflex nature of these evoked responses (6, 14).

Selectivity of the electrical stimulation to specific spinal regions and excitability to recruitment of motor pools were suggested to be important for enhancing rehabilitation effects after SCI (9, 10, 17). It has recently been demonstrated that continuous cervical tSCS may selectively yield independent and coordinated movements in proximal and distal upper-limb joints (18). In addition, cervical tSCS was shown to elicit postactivation depression in the spinally evoked motor responses with both intact (14, 19) and SCI (20) individuals. Various cervical tSCS configurations have been used for targeting upper-limb muscles. Cathode electrodes were typically configured medially over the C3-T4 vertebral regions on the posterior side of the neck (4, 5, 14, 20), whereas the upper-limb motor pools were suggested to be arranged rostral to T1 vertebra (21–23). Anode electrodes were placed over the anterior neck (14, 20), clavicles (24, 25), iliac crests (2–5), or the back (26, 27). However, since these studies applied cervical tSCS for different proposes (e.g., SCI rehabilitation or for assessment of motor responses), as well as with different stimulation paradigms (e.g., trains of pulses or single pulses), direct comparison between electrode configurations is not possible. Furthermore, selectivity and excitability of electrode configurations on the transsynaptic activation of the upper-limb muscles have not been examined. Better understanding of the evoked responses can inform methodological considerations to help optimize recruitment of Ia afferents.

In the present study, we therefore assessed spinally evoked muscle responses in multiple upper-limb muscles with cervical tSCS delivered using different cathode and anode electrode configurations. First, postactivation depression in the evoked responses was confirmed in all analyzed muscles for the cathode electrode placed over C6, C7, and T1 vertebral levels, whereas the anode was fixed over the anterior neck. The selectivity of spinal regions and excitability to the recruitment of motoneurons during cervical tSCS were then compared between the three cathode configurations using recruitment curves (*study 1*). Specifically, in this study, selectivity is referred to as activation of motor pools in different spinal regions using different cathode locations (C6, C7, and T1), and excitability as the susceptibility to which motoneurons are recruited during cervical tSCS. In a separate protocol (*study 2*), four anode configurations were compared by varying the anodes over the anterior neck (14, 20), distal end of clavicles (24, 25), iliac crests (2–5), or the back (26, 27).

Based on theoretical mechanisms underlying motor activation during tSCS and previous experimental studies, we hypothesized that postactivation depression would be observed in all muscles for all cathode configurations. Moreover, based on the anatomy and myotome maps of the cervical spinal cord (22, 23), we further hypothesized that tSCS would preferentially evoke responses in proximal arm muscles with cathode configured more rostrally over the C6 level, and distal hand muscles with cathodes more caudally, over T1 level. Specifically, considering the organization of hand muscles motor pools in more caudal spinal levels compared with the arm muscles (23), the use of relatively large cathode electrodes placed over the C6 vertebra (overlapping C6 and C7 spinal levels) and T1 vertebra (overlapping C8 and T1 spinal levels) was therefore expected to yield different levels of activation of distal and proximal upper-limb muscles. Moreover, placing the cathode electrode over C7 vertebra (overlapping C7 and C8 spinal levels) would serve as an intermediate level for confirming the selectivity of distal and proximal muscles when the cathode is varied to rostral (C6) and caudal (T1) levels. This would be analogous to what has been demonstrated with lumbar tSCS in the lower-limb muscles (15, 28–30). We further hypothesized that greater recruitment of upper-limb muscles would be yielded by configuring the anode over the anterior neck (14, 20) due to the proximity to the cathode, which may maximize the electric field flow across the spinal cord.

METHODS

Participants

Ten able-bodied male individuals were recruited for this study. The age, weight, and height of the participants were 25.8 ± 2.6 yr, 68.8 ± 8.3 kg, and 173.4 ± 5.1 cm (means ± SD), respectively. All participants were right-handed in accordance with the Edinburgh Handedness Inventory (scores across participants were between 0.55 and 1, where 1 indicates completely right-handed and −1 indicates completely left-handed) (31). None of the participants had a history of neurological and/or musculoskeletal impairments. All participants gave written informed consent in accordance with the Declaration of Helsinki before participating in the study. The experimental procedures were approved by the local institutional ethics committee of the Graduate School of Arts and Science at The University of Tokyo.

Data Acquisition

Electromyographic (EMG) signals were recorded using Ag/AgCl surface electrodes (Vitrode F-150S, Nihon Kohden, Tokyo, Japan) simultaneously from upper-limb muscles on the right (dominant) hand, since handedness and hand dominance may affect motor responses (32–34). Electromyographic signals from six muscles innervated by cervical spinal levels were recorded on: *1*) biceps brachii (BB), innervated by C5-C6 spinal levels; *2*) triceps brachii (TB), innervated by C6-T1 spinal levels; *3*) flexor carpi radialis (FCR), innervated by C6-C7 spinal levels; *4*) extensor carpi radialis (ECR), innervated by C5-T1 spinal levels; *5*) first dorsal interosseous (FDI), innervated by C5-T1 spinal levels; and *6*) abductor pollicis brevis (APB), innervated by C5-T1 spinal levels (14, 23). Specifically, two electrodes were placed over the belly of each muscle with an interelectrode distance of ~20 mm, whereas the ground electrode was placed around the lateral epicondyle (14). Prior to application of electrodes, the skin was cleaned using alcohol to reduce skin impedance.

All EMG signals were amplified (×1,000) using a bipolar configuration and band-pass filtered between 5 and 1,000 Hz using a multichannel EMG amplifier (MEG-6108, Nihon

Kohden, Tokyo, Japan). Moreover, the EMG signals were digitized at a sampling frequency of 4,000 Hz using an analog-to-digital converter (Powerlab/16SP, ADInstruments, Castle Hill, Australia) and stored on the computer for postprocessing.

Experimental Protocol

During the experiment, participants remained at rest in the supine position with both arms resting on the bed along the body (Fig. 1A). A small pillow was placed under the neck to ensure that the head was rested comfortably and that tSCS electrodes remained fixed. The tSCS stimuli were applied by delivering two monophasic pulses with an interstimuli interval of 50 ms of equal pulse amplitudes and 2 ms pulse width (14) using a constant current electrical stimulator (DS7A, Digitimer, Welwyn Garden City, UK). The two evoked responses elicited by the stimuli were recorded at each muscle simultaneously. For each participant, the experimental protocol of *study 2* was conducted following *study 1* in a single experimental session, whereas at least 10-min rest was given between experiments.

Cathode electrode configurations (study 1).

Study 1 was conducted to confirm postactivation of evoked responses in multiple upper-limb muscles with different cathode electrode configurations, and to further investigate the selectivity to spinal regions and excitability of recruitment of motoneurons during cervical tSCS. Three configurations were compared by positioning the cathode electrode (5 × 5 cm) on the skin surface of the posterior side of the neck centered over the spinous process of: *1*) C6; *2*) C7; and *3*) T1 vertebrae, while the anode electrode (7.5 × 10 cm; horizontally positioned) remained fixed along the midline on the anterior side of the neck (Fig. 1A), consistent to Milosevic et al. (14). Specifically, stimulating pulses were applied (see *Experimental Protocol*) and the stimulating current amplitude was varied from 10 to 100 mA, in 10 mA increments (29, 35). Large size electrodes were used to alleviate the pain felt by the participants during the stimulation. Nonetheless, the maximal current amplitude stimulated in two participants was below 100 mA (90 mA and 80 mA) due to discomfort during stimulation. For all participants, three responses (36) were recorded for each stimulation amplitude with intervals of 10–15 s to obtain the recruitment curves as depicted in the Fig. 2 for each muscle (BB, TB, FCR, ECR, FDI, and APB) and each cathode configuration (C6, C7, and T1), analogous to a previous study examining lower-limb muscles (30). The order of cathode configurations (C6, C7, and T1) was randomized between participants, and a break of at least 3 min was administered between conditions.

Anode electrode configurations (study 2).

After completion of the *study 1* experimental protocol, a cathode location (C6, C7, or T1) and stimulation amplitude were chosen for each subject to be used in the subsequent experiments of *study 2*. The experimenter identified the cathode location and stimulation intensity, which could yield a suppression of the second responses in relation to the first (i.e., postactivation depression) simultaneously in all muscles by visual inspection of the data recorded during *study 1*. Specifically, the location and stimulation amplitude were chosen to be on the ascending part of the recruitment curve, when the second response had a smaller peak-to-peak amplitude than the first response simultaneously for all six muscles, as previously described by Milosevic et al. (14). The chosen cathode location and stimulus amplitude were then used for experiments in *study 2* (cathode location C6: n = 0, C7: n = 2, T1: n = 8; current amplitude means ± SD: 65.0 ± 10.8 mA). These locations are similar to those used previously when the anode was configured over the neck (14), shoulders (24), iliac crests (5), and the back (26). The choice of the cathode location and stimulus amplitude was confirmed in postprocessing [see RESULTS: *Anode Electrode Configurations (study 2)*].

Study 2 was conducted to investigate postactivation depression in different anode electrode configurations elicited in

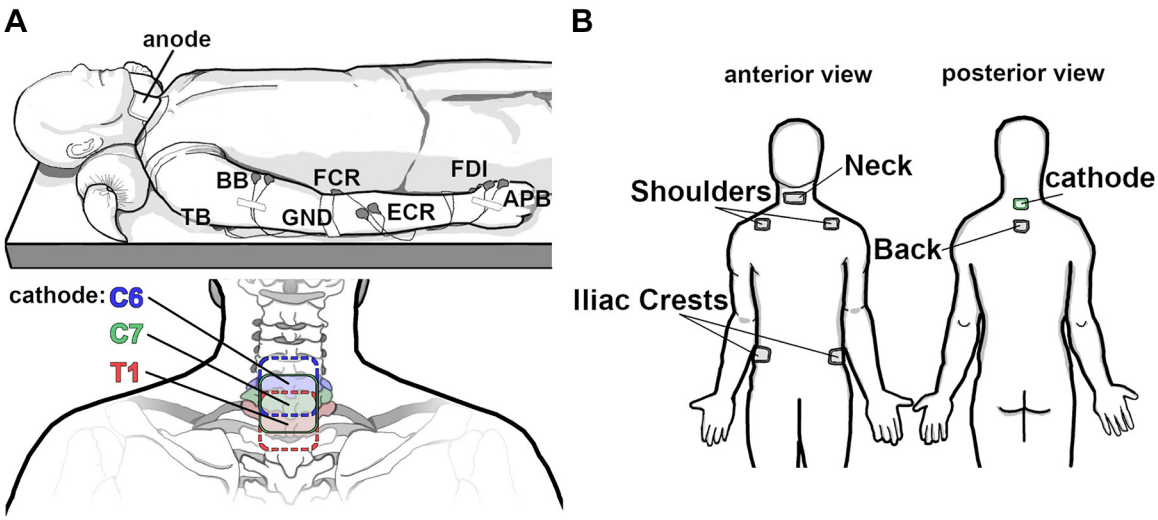

Figure 1. Illustration of the experimental setups of *study 1* (*A*) and *study 2* (*B*). The upper image of *A* illustrates the cervical tSCS applied with anode placed over the anterior neck, whereas the EMG signals were recorded from biceps brachii (BB), triceps brachii (TB), flexor carpi radialis (FCR), extensor carpi radialis (ECR), first dorsal interosseous and abductor pollicis brevis (APB), while the ground electrode (GND) was fixed around the elbow. In the bottom image of *A*, the configuration of the cathode electrode over C6, C7, and T1 vertebral levels are shown. In *B*, the Neck, Shoulders, Iliac Crests, and Back configurations of anodes are illustrated.

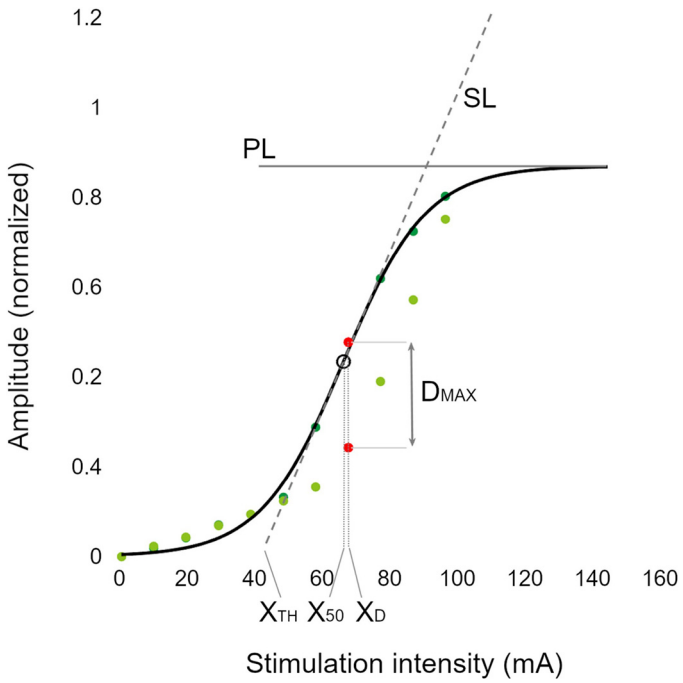

Figure 2. Boltzmann sigmoid function fitted to the recruitment curve (black line) of the peak-to-peak amplitude of the first responses (dark green circles) of a representative muscle evoked using cervical tSCS stimulating currents from 10 mA to 100 mA (increments of 10 mA) with the cathode electrode placed over the C7 vertebral level. The parameters extracted from the sigmoid fit: slope (*SL*), plateau (*PL*), stimulus intensity at 50% of the plateau (X_{50}), and threshold stimulus intensity (X_{TH}) are indicated. Additionally, the second evoked responses (light green circles) are shown. Using the peak-to-peak amplitude of the first and second responses, the maximal normalized suppression (D_{MAX}) and the current intensity where the maximal suppression occurred (X_D) are indicated. For each stimulation intensity, each a pair of data points consists of average peak-to-peak values of three pairs of stimulation pulses (50-ms interstimuli interval). Comparisons were performed between different upper-limb muscles (BB, TB, FCR, ECR, FDI, and APB) and different cathode locations (C6, C7, and T1). APB, abductor pollicis brevis; BB, biceps brachii; ECR, extensor carpi radialis; FCR, flexor carpi radialis; FDI, first dorsal interosseous; TB, triceps brachii.

multiple upper-limb muscles. Two monophasic pulses were applied (see *Experimental Protocol*) at the chosen cathode location and stimulus amplitude to compare the four different anode configurations illustrated in Fig. 1*B*: *1*) one anode electrode (7.5 × 10 cm) located on the midline of the anterior side of the neck (Neck) (14, 20); *2*) two anode electrodes (5 × 5 cm) located bilaterally over the distal end of the clavicles (Shoulders) (24, 25); *3*) two anode electrodes (5 × 5 cm) located bilaterally over the iliac crests (Iliac Crests) (2–5); and *4*) one anode electrode (5 × 5 cm) located ~4 cm below the cathode electrode on the posterior side of the neck (Back) (26, 27). Three responses (36) for each anode configuration were recorded with intervals of 10–15 s. The order of conditions (Neck, Shoulders, Iliac Crests, and Back) was randomized between participants and a break of at least 3 min was administered between conditions.

A numeric rating scale (NRS) was used to evaluate self-reported pain from 0 to 10, where 0 corresponds to "no pain" and 10 corresponds the "worst pain imaginable" (37). The pain level was evaluated by showing participants a visual analog scale and asking them to rate the pain experienced during stimulation delivered with each anode configuration immediately after each protocol (Neck, Shoulder, Iliac Crest, and Back).

Data Analysis

In postprocessing, which was performed using a custom written MATLAB script (MathWorks, Natick, MA), the peak-to-peak amplitudes were measured from the first and second evoked responses to the pair of pulses of each muscle. The peak-to-peak amplitude of the first and second responses within three pairs of pulses delivered for each stimulus amplitude was averaged (36). The averaged values were then used to analyze the activation of upper-limb muscles for different cathode (*study 1*) and anode (*study 2*) electrode configurations.

Cathode electrode configuration.

Postactivation depression. To evaluate tSCS postactivation depression in the second responses compared with the first (14, 15, 38, 39) for different cathode locations (C6, C7, and T1) using data obtained in *study 1*, the following parameters were analyzed (Fig. 2): *1*) peak-to-peak amplitudes of the first and second responses at their maximum difference were compared across cathode configurations for each muscle individually; *2*) maximum normalized difference of the second peak-to-peak evoked response compared with the first response (D_{MAX}), which was calculated as $D_{MAX} = max((F[X] - S[X])/F[X])$, where $F[X]$ and $S[X]$ correspond to the first and second experimentally obtained responses at X = 10, …, 100 mA; and *3*) stimulus intensity at the maximum postactivation depression (X_D), which was the stimulating current intensity at D_{MAX}. These variables, which represent the maximal normalized postactivation depression on the recruitment curve (D_{MAX}) and the corresponding stimulus intensity of the maximal postactivation depression (X_D), were compared between muscles and cathode configurations.

Recruitment curves. In *study 1*, for each cathode configuration (C6, C7, and T1 levels, whereas the anode was fixed on the anterior side of the neck), the average peak-to-peak amplitudes obtained for each stimulation intensity (10 to 100 mA, in 10 mA increments) were used to obtain the recruitment curve of the first responses for each muscle (BB, TB, FCR, ECR, FDI, and APB) for each participant. Specifically, data for each recruitment curve were first normalized to the maximum value elicited between the three cathodes configurations. The signal-to-noise ratio of these responses were compared between muscles, and the results showed no statistically significant differences [$F(5,45) = 1.81$, $P = 0.130$]. Normalized responses were then fitted using a Boltzmann sigmoidal function (12, 40, 41):

$$RC(x) = \frac{PL}{1 + e^{\frac{(X_{50} - x)}{K}}}$$

where the recruitment curve, RC, is a function of the stimulus intensity, x, whereas parameter PL is the function's maximum value (plateau), X_{50} is the stimulus intensity at 50% of the plateau value, and K is a slope parameter. For sigmoid fits that yielded the plateau value greater than 2 (i.e., fits that extrapolated features not implicitly represented by the experimental data), data were re-fitted by defining X_{50} = 100

mA as the initial condition for the fitting (23 out of 180 cases). If the sigmoid functions plateau still remained greater than 2 after re-fitting, the data were discarded from the analysis (4 out of 180 cases) as it was deemed that the fit could not represent the data. Moreover, it was verified that the coefficient of determination (R^2) was greater than 0.9 for each sigmoid fit (mean ± SD: 0.99 ± 0.01) (40, 42, 43). After the recruitment curve functions were obtained, four parameters were extracted from each fit, as shown in Fig. 2: *1*) threshold stimulus intensity to motor activation (X_{TH}), indicating the excitability to the initial recruitment of motoneurons; *2*) maximum slope (*SL*), indicating the excitability to the recruitment of motoneurons with the increase of stimulation current amplitude; *3*) stimulus intensity at 50% of the plateau (X_{50}), serving as a comparative index between the excitability to the initial recruitment of motoneurons (X_{TH}) and the increase of current amplitude (*SL*); and *4*) plateau (*PL*), indicating the total motor output. The parameters *PL* and X_{50} were obtained from the output of the fitting algorithm, *SL* was calculated as *PL/4K*, and X_{TH} was obtained from the line equation defined by X_{50}, PL/2, and *SL*, as described previously (12, 40–42).The selectivity of activation of different upper-limb muscles was compared between cathode configurations (C6, C7, and T1) through the excitability parameters *SL*, X_{50}, and X_{TH} and motor output parameter, *PL*.

Anode electrode configurations.

First, the postactivation depression in the second responses elicited at the stimulus intensity and cathode location chosen by the experimenter for each participant to be used in *study 2* [see *Experimental Protocol: Anode electrode configurations (study 2)*] was confirmed in using data recorded in *study 1*. Since postprocessing confirmed correct selection of stimulus intensity and cathode location parameters [(see RESULTS: *Anode electrode configurations (study 2)*], the peak-to-peak amplitudes of the first and second responses elicited with different anode configurations (Neck, Shoulders, Iliac Crests, and Back) were compared with evaluate effects of different anode configurations on the transsynaptic activation of each muscle in *study 2*.

Statistics

First, for each muscle separately, a within-subjects design two-way ANOVA was used to compare the peak-to-peak amplitudes of the first and second responses at maximum suppression (postactivation depression: first and second response) between cathode configurations (cathode: C6, C7, and T1). In addition, to compare postactivation depression, D_{MAX} and X_D were also analyzed using a within-subjects design two-way ANOVA to compare responses between muscles (muscle: BB, TB, FCR, ECR, FDI, and APB) and different cathode locations (cathode: C6, C7, and T1). The selectivity of activation of upper-limb muscle motor pools with different cathode configurations was analyzed by comparing excitability parameters *SL*, X_{50}, and X_{TH} and motor output parameter, *PL*, using a within-subjects design two-way ANOVA between cathode locations (cathode: C6, C7, and T1) across different muscles (muscle: BB, TB, FCR, ECR, FDI, and APB).

The postactivation depression in the second responses elicited with stimulus intensity and cathode configurations used for each participant in *study 2* [*Experimental Protocol: Anode electrode configurations* (*study 2*)] was analyzed using a *t* test to compare the first and second response amplitudes for each muscle separately. In *study 2*, a within-subject design two-way ANOVA was used to compare different anode configurations (anode: Neck, Shoulder, Iliac Crests, and Back) and suppression of the second response compared with the first (postactivation depression: first and second response) for each muscle separately.

When significant interactions were found on the two-way ANOVA, a within-subject design one-way ANOVA (or a *t* test) was performed for each factor separately. Post hoc multiple comparisons were conducted when significant ANOVA results were found and adjusted using the Bonferroni correction factor. Greenhouse–Geisser correction was used when the sphericity assumption was violated, which was confirmed using the Mauchly's test. Normality of data distributed was tested using the Shapiro–Wilk's test before performing the analysis. Although most of the data were found to be normally distributed, the results of non-normally distributed data were confirmed using the non-parametric equivalent Friedman's test and Wilcoxon test. Furthermore, the NRS scores for different anode configurations were compared using Friedman's test, since it is an ordinal variable. All statistical tests were performed using SPSS (IBM, Armonk, NY) with a significance level of $\alpha = 0.05$.

RESULTS

Cathode Electrode Configurations (study 1)

Averaged evoked responses of a representative participant in *study 1* for different cathode configurations (C6, C7, and T1) across stimulus intensities varying from 10 to 100 mA are shown in Fig. 3. For this representative participant, postactivation depression can be seen in most muscles. Distal hand muscles (FDI and APB) were preferentially activated when the cathode was placed over T1 compared with C6 and C7 vertebral levels, while that was not true for the proximal arm muscles (BB, TB, FCR, and ECR). Moreover, higher stimulation intensities were required to elicit responses in distal muscles (FDI and APB) compared with proximal muscles (BB, TB, FCR, and ECR).

Postactivation depression. Results obtained from the comparison of the maximum peak-to-peak amplitude difference between the second and first responses (postactivation depression: first vs. second responses) with three cathode configurations (cathode: C6, C7, and T1) for each muscle are summarized in Fig. 4, whereas Table 1 shows the main statistical results. For BB, TB, FCR, and ECR, two-way ANOVA showed no significant interactions and statistically significant main effect for postactivation depression, but not for cathode comparisons. For FDI and APB, since interactions were shown, follow-up analyses with one-way ANOVA or *t* tests indicate statistically significant postactivation depression for all cathode configurations; moreover, cathode comparisons showed that the first and second responses were different for the APB muscle only. In Fig. 4, post hoc multiple comparisons further indicate differences in the first and second responses between C6 and T1 for the APB muscle.

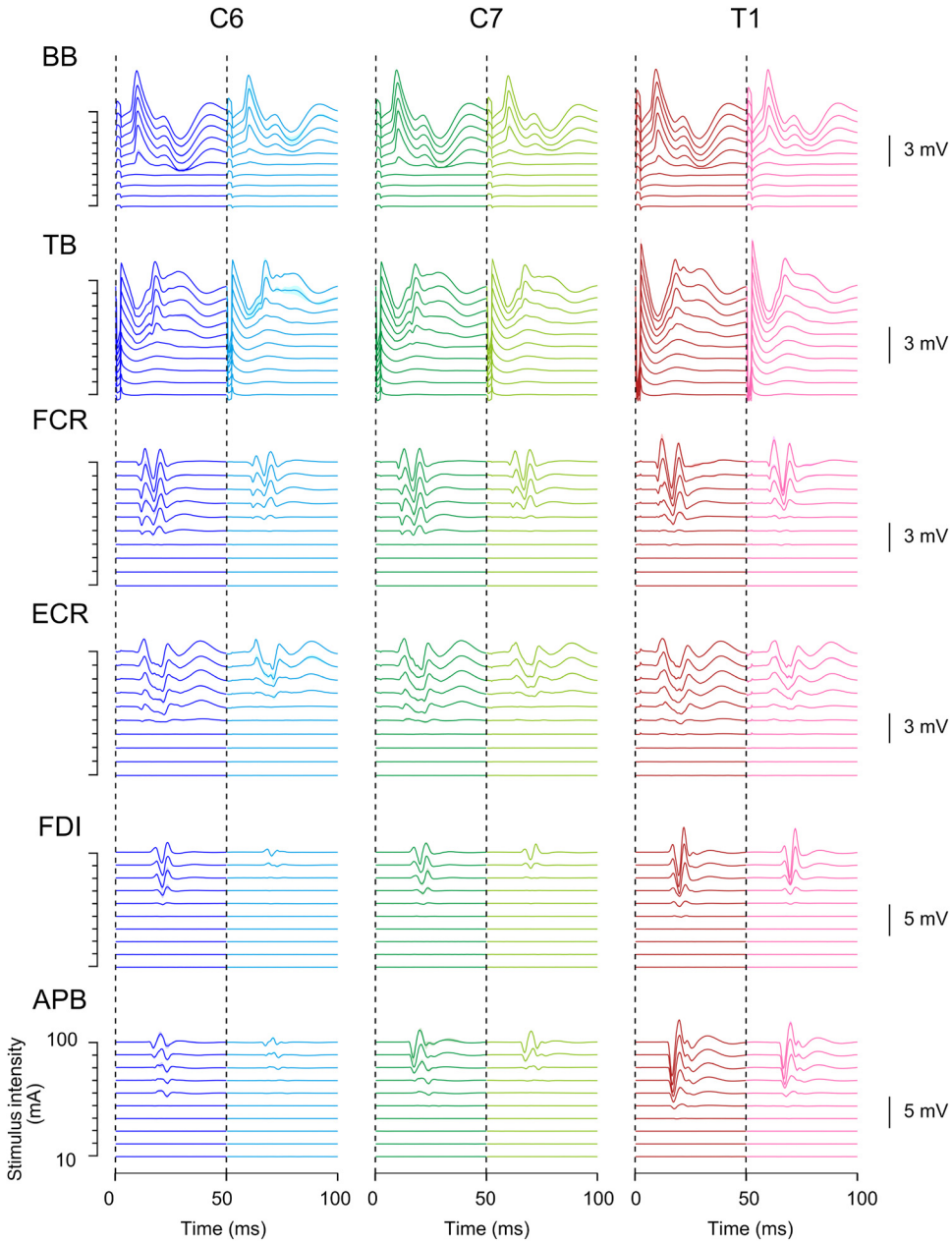

Figure 3. Representative participant averaged responses evoked in the six muscles (BB, TB, FCR, ECR, FDI, and APB) using cervical tSCS with the anode was placed over the anterior neck and the cathode placed over C6, C7, and T1 vertebral levels. Three responses elicited with stimulations delivered as two monophasic pulses (50-ms interstimuli interval) were averaged for each stimulation amplitude (from 10 mA to 100 mA, in increments of 10 mA) and cathode configuration. The first and second averaged responses elicited with the cathode placed over C6, C7, and T1 are shown for each muscle. Each trace corresponds to the averaged EMG time series with amplitudes varying from 10 mA (*bottom*) to 100 mA (*top*), where the darker shade color indicates the first elicited response and the lighter shade color the second response. The shaded areas in the corresponding colors indicate the standard deviation of the three responses. The dotted lines indicate the instant at which the first and second stimuli were delivered. APB, abductor pollicis brevis; BB, biceps brachii; ECR, extensor carpi radialis; FCR, flexor carpi radialis; FDI, first dorsal interosseous; TB, triceps brachii.

Results obtained from the analyses of the two parameters examined for the maximum postactivation depression (D_{MAX} and X_D) are summarized in Fig. 5*A*, whereas Table 2 summarizes the main statistical results. For both D_{MAX} and X_D, the two-way ANOVA showed no significant interactions and statistically significant main effects for muscle, but not for cathode comparisons. In Fig. 5*A*, post hoc multiple comparisons between muscles indicated differences between BB and TB for D_{MAX} (NOTE: despite statistical significance in the two-way ANOVA for X_D, post hoc analyses with Bonferroni correction did not show significant differences).

Recruitment curves. Results obtained from the analyses of the four parameters extracted from the sigmoid fits of the recruitment curves: *SL*, *PL*, X_{TH}, and X_{50} are summarized in Fig. 5*B*, whereas Table 2 summarizes the main statistical results. For *SL*, *PL*, X_{TH}, and X_{50}, since interactions were shown, follow-up analyses with one-way ANOVA indicate mostly significant differences between cathodes for the FDI and APB muscles; moreover, muscle comparisons showed mostly significant differences for X_{TH} and X_{50}. In Fig. 5*B*, post hoc multiple comparisons showed significant differences between cathodes configurations indicating that distal hand muscles (FDI and APB) were preferentially activated when the cathode was placed over T1 compared with C6 and C7 vertebral levels (c.f. *PL* in Fig. 5*B*), whereas this was not true for the proximal arm muscles (BB, TB, FCR, and ECR) (NOTE: despite statistical

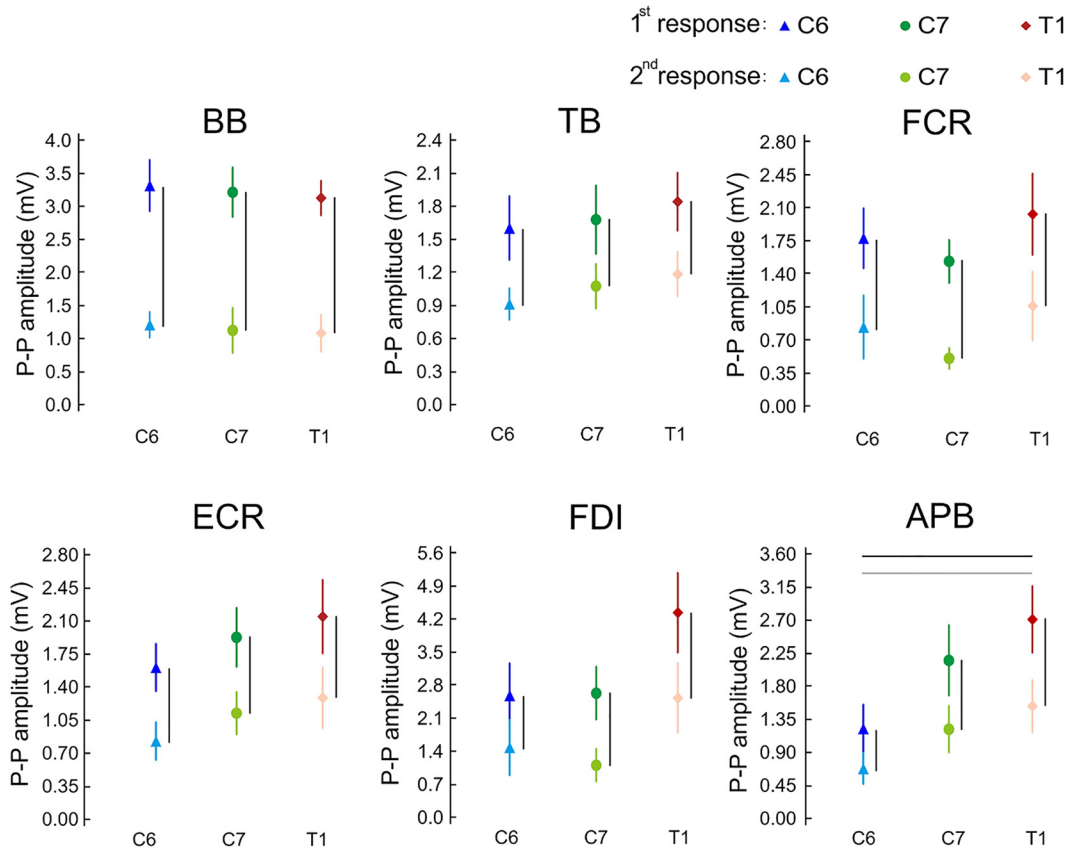

Figure 4. The mean values of the responses at the maximal suppression point are indicated with blue triangles, green circles, and red diamonds for C6, C7, and T1, respectively. Shown are the corresponding standard error vertical bars. The sample size of each data sets is $n = 10$ participants. The dark shades represent the first responses, and the light shades represent the second responses. Significant differences between cathode configurations are indicated with black and gray bars for the first and second responses, respectively. Significant differences between the first and second responses are indicated with vertical black bars. APB, abductor pollicis brevis; BB, biceps brachii; ECR, extensor carpi radialis; FCR, flexor carpi radialis; FDI, first dorsal interosseous; TB, triceps brachii.

significance in the one-way ANOVA for PL and X_{TH} across muscles, and for X_{TH} and X_{50} across different cathodes configurations, post hoc analyses with Bonferroni correction did not show significant differences).

Anode Electrode Configurations (study 2)

Suppression of the second responses compared with the first elicited using the cathode configurations and stimulus

Table 1. *Statistical analyses results showing within-subject two-way ANOVA interactions and main effect results for postactivation depression (first and second responses) and cathode configurations (C6, C7, and T1) comparisons of the responses evoked in each muscle (BB, TB, FCR, ECR, FDI, and APB) separately*

		Postactivation depression			Cathode	
	Interaction	C6	C7	T1	First	Second
BB	$F(2,18) = 0.1$ $P = 0.872$		**$F(1,9) = 35.1$** **$P < 0.001$**		$F(2,18) = 0.2$ $P = 0.799$	
TB	$F(2,18) = 0.7$ $P = 0.526$		**$F(1,9) = 13.2$** **$P = 0.005$**		$F(2,18) = 0.8$ $P = 0.454$	
FCR	$F(2,18) = 0.5$ $P = 0.646$		**$F(1,9) = 28.7$** **$P < 0.001$**		$F(2,18) = 2.5$ $P = 0.114$	
ECR	$F(1.2,10.9) = 0.3$ $P = 0.618$		**$F(1,9) = 26.8$** **$P < 0.001$**		$F(2,18) = 1.6$ $P = 0.237$	
FDI	**$F(2,18) = 5.4$** **$P = 0.015$**	**$t(9) = 4.2$** **$P = 0.002$**	**$t(9) = 5.2$** **$P < 0.001$**	**$t(9) = 6.3$** **$P < 0.001$**	$F(2,18) = 2.9$ $P = 0.080$	$F(2,18) = 2.3$ $P = 0.128$
APB	**$F(1.2,10.6) = 8.8$** **$P = 0.011$**	**$t(9) = 3.3$** **$P = 0.009$**	**$t(9) = 4.4$** **$P = 0.002$**	**$t(9) = 5.0$** **$P < 0.001$**	**$F(2,18) = 9.3$** **$P = 0.002$**	**$F(2,18) = 4.2$** **$P = 0.031$**

When interaction was significant, the factors were compared separately with within subject one-way ANOVA or a t test. Greenhouse–Geisser correction was used when the sphericity assumption was violated. The P values in bold indicate significant differences for a significance level of $\alpha = 0.05$. APB, abductor pollicis brevis; BB, biceps brachii; ECR, extensor carpi radialis; FCR, flexor carpi radialis; FDI, first dorsal interosseous; TB, triceps brachii.

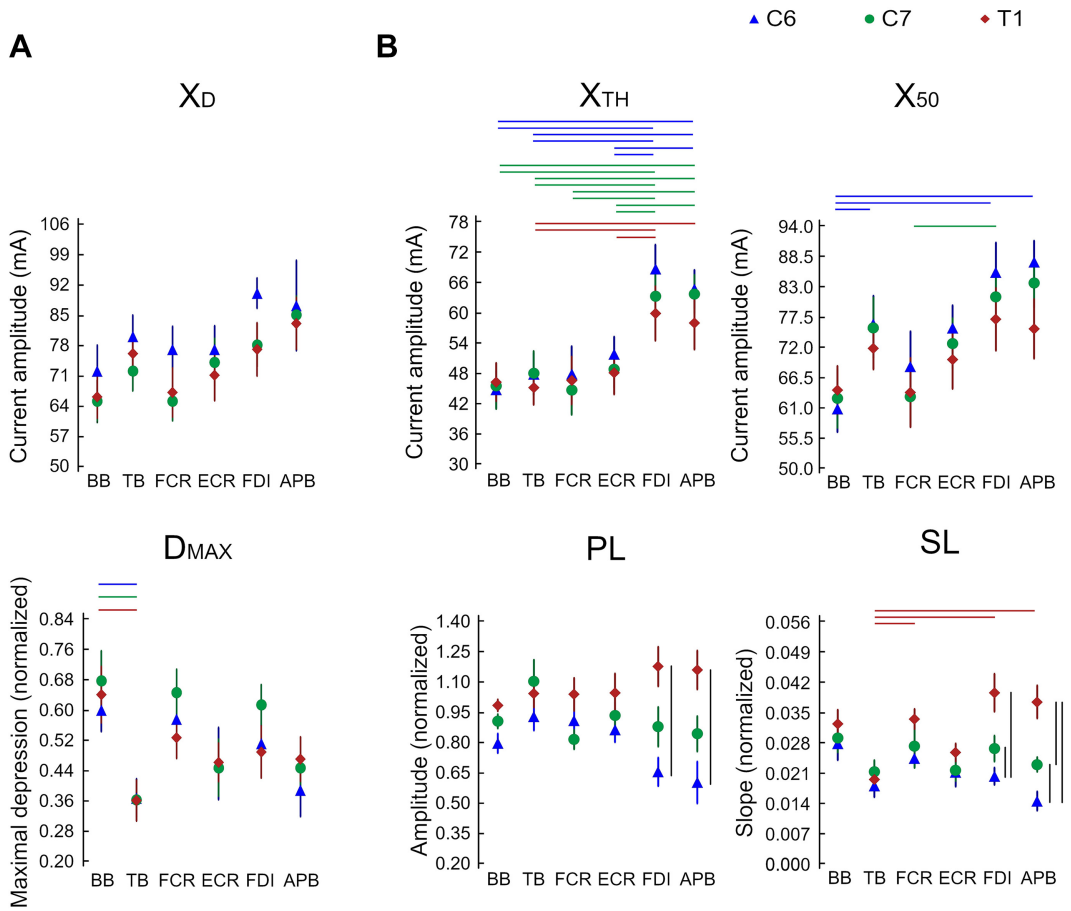

Figure 5. *A*: postactivation depression (*study 1*): parameters computed from the difference between the peak-to-peak values of the first and second responses (X_D and D_{MAX}) compared for the six muscles (BB, TB, FCR, ECR, FDI, and APB) and the three cathodes configurations (C6, C7, and T1). The sample sizes of the parameters X_D and D_{MAX} are $n = 10$ participants. *B*: cathode configuration (*study 1*): parameters obtained from the fits of the recruitment curves of the first responses (SL, PL, X_{50}, and X_{TH}) compared for six muscles and three cathode configurations. The sample sizes of the parameters SL, PL, X_{50}, and X_{TH} are $n = 9$ participants. The mean values of each variable are indicated with blue triangles, green circles, and red diamonds for C6, C7, and T1, respectively. Shown are the corresponding standard error vertical bars. Significant differences between muscles are indicated with blue, green, and red horizontal bars representing C6, C7, and T1 cathode configurations, respectively. Significant differences between cathodes configurations are indicated with vertical black bars. APB, abductor pollicis brevis; BB, biceps brachii; ECR, extensor carpi radialis; FCR, flexor carpi radialis; FDI, first dorsal interosseous; TB, triceps brachii.

intensity that were chosen for each participant to be used in *study 2* [see *Experimental Protocol: Anode electrode configurations (study 2)*] were confirmed using *t* tests for each muscle [BB: $t(9) = 4.8$, $P < 0.001$; TB: $t(9) = 3.7$, $P = 0.005$; FCR: $t(9) = 3.9$, $P = 0.004$; ECR: $t(9) = 3.6$, $P = 0.005$; FDI: $t(9) = 3.4$, $P = 0.008$; APB: $t(9) = 2.8$, $P = 0.019$].

Averaged first and second evoked responses of a representative participant in *study 2* for different anode configurations (Neck, Shoulder, Iliac Crest, and Back) are shown in Fig. 6. For this representative participant, the largest responses were recorded with the Neck anode in all muscles, except TB, whereas the smallest responses were recorded with the Back anode.

Results obtained from the comparison of the peak-to-peak amplitude of the second response compared with the first (postactivation depression) with three anode configurations (Neck, Shoulder, Iliac Crest, and Back) elicited with the stimulation intensity chosen by the experimenter for each muscle are summarized in Fig. 7, whereas Table 3 summarizes the main statistical results. For FCR, the two-way ANOVA showed no significant interactions and statistically significant main effects for anode, but not for postactivation depression comparisons. For BB, TB, ECR, FDI, and APB, since interactions were shown, follow-up analyses with one-way ANOVA or *t* tests indicate statistically significant postactivation depression mostly for the Neck anode configuration; moreover, anode comparisons showed that the first and second responses were different for most muscles. In Fig. 7, post hoc multiple comparisons further indicated mostly differences between the Neck first and second responses elicited with those of the Iliac Crest and Back anode configuration in all muscles except for FDI (NOTE: despite statistical significance between anode factor in the one-way ANOVA for first responses from FDI and second responses from BB, post hoc analyses with Bonferroni correction did not show significant differences; significant effects for postactivation factor at APB obtained for the Shoulder and Back anode configurations were not confirmed using nonparametric tests).

The NRS self-reported discomfort scores across participant for different anode configurations were Neck: 3.5 ± 1.6,

Table 2. *Statistical analyses results showing within subject two-way ANOVA interactions and main effect results for cathode (C6, C7, and T1) and muscle (BB, TB, FCR, ECR, FDI, and APB) comparisons of postactivation depression (D_{MAX} and X_D) and recruitment curve parameters (SL, PL, X_{50}, and X_{TH})*

		Cathode						Muscle		
	Interaction	Bb	TB	FCR	ECR	FDI	APB	C6	C7	T1
D_{MAX}	$F(10,90) = 1.0$ $P = 0.453$			$F(2,18) = 2.2$ $P = 0.144$					**$F(5,45) = 6.0$** $P < 0.001$	
X_D	$F(3.0,26.9) = 0.8$ $P = 0.502$			$F(1.3,11.5) = 2.0$ $P = 0.183$					**$F(3.0,27.1) = 3.8$** $P = 0.032$	
SL	**$F(10,80) = 4.0$ $P < 0.001$**	$F(1.2,10.9) = 0.4$ $P = 0.574$	$F(2,16) = 0.8$ $P = 0.478$	$F(1.2,11.2) = 1.8$ $P = 0.201$	$F(1.2,9.9) = 0.9$ $P = 0.381$	**$F(2,16) = 13.3$ $P < 0.001$**	**$F(2,16) = 18.8$ $P < 0.001$**	$F(1.8,14.6) = 3.0$ $P = 0.084$	$F(1.7,15.7) = 1.2$ $P = 0.314$	**$F(5,40) = 6.2$ $P < 0.001$**
PL	**$F(10,80) = 2.2$ $P = 0.025$**	**$F(2,18) = 4.4$ $P = 0.028$**	$F(2,16) = 1.0$ $P = 0.387$	$F(2,18) = 1.5$ $P = 0.242$	$F(2,16) = 1.2$ $P = 0.321$	**$F(2,16) = 8.4$ $P = 0.003$**	**$F(2,16) = 7.5$ $P = 0.005$**	**$F(5,40) = 2.9$ $P = 0.025$**	$F(5, 45)=1.7$ $P = 0.158$	$F(2.5,19.8) = 1.1$ $P = 0.345$
X_{50}	**$F(10,80) = 1.9$ $P = 0.049$**	$F(2,18) = 1.0$ $P = 0.385$	$F(2,16) = 1.2$ $P = 0.323$	$F(1.2,11.2) = 1.0$ $P = 0.339$	$F(2,16) = 1.2$ $P = 0.336$	$F(2,16) = 2.5$ $P = 0.109$	**$F(2,16) = 5.1$ $P = 0.019$**	**$F(5,40) = 7.9$ $P < 0.001$**	**$F(5, 45) = 6.6$ $P < 0.001$**	**$F(5,40) = 3.3$ $P < 0.001$**
X_{TH}	**$F(10,80) = 2.0$ $P = 0.039$**	$F(2,18) = 0.4$ $P = 0.666$	$F(2,16) = 0.9$ $P = 0.420$	$F(2,18) = 0.5$ $P = 0.618$	$F(2,16) = 1.8$ $P = 0.198$	**$F(2,16) = 5.7$ $P = 0.013$**	$F(2,16) = 2.4$ $P = 0.124$	**$F(5,40) = 16.0$ $P < 0.001$**	**$F(2.7,24.4) = 12.4$ $P < 0.001$**	**$F(5,40) = 8.9$ $P < 0.001$**

When interaction was significant, the factors were compared separately with within-subject one-way ANOVA. Greenhouse–Geisser correction was used when the sphericity assumption was violated. The *P* values in bold indicate significant differences for a significance level of $\alpha = 0.05$. APB, abductor pollicis brevis; BB, biceps brachii; ECR, extensor carpi radialis; FCR, flexor carpi radialis; FDI, first dorsal interosseous; TB, triceps brachii.

Shoulders: 3.5 ± 1.5, Iliac Crests: 3.2 ± 1.5, Back: 3.7 ± 1.9 (mean ± SD). Note that all participants reported a discomfort score of zero at the start of the study. Friedman's test showed no significant differences in the scores for different anode configurations [χ^2 (3, 10) =1.8, $P = 0.606$].

DISCUSSION

In this study, we showed postactivation depression in multiple muscles with all three cathode configurations (C6, C7, and T1). Moreover, we demonstrated that distal (FDI and APB) and proximal (BB, TB, FCR, and ECR) upper-limb muscles had different activation excitability elicited by tSCS with different cathode configurations. Specifically, distal hand muscles were preferentially activated with the cathode configured over the T1 vertebra compared with C6 and C7 configurations, whereas there was no selectivity for proximal arm muscles. Activation of distal hand muscles also required higher stimulation intensities compared with proximal arm muscles. Furthermore, larger responses were elicited with the Neck anode than other anode configurations (Iliac Crests, Shoulders, and Back), whereas the levels of discomfort were similar. Although postactivation depression in the elicited responses was achieved with anode configurations in multiple muscles, the Neck configuration may elicit transsynaptic and direct motor activation during cervical tSCS with less current amplitude.

Postactivation Depression in the Spinally Evoked Motor Responses during Cervical tSCS

Transcutaneous spinal cord stimulation can elicit motor responses in muscles through activation of motoneurons via monosynaptic and oligosynaptic pathways with sensory fibers or interneurons and/or through direct excitation of motor axons in the ventral roots of the spinal cord (6, 15, 38). Primarily, the contribution of monosynaptic Ia excitation to the recruitment of α-motoneurons has been suggested when assessed using paired stimuli by examining the magnitude of suppression of the conditioned (second) evoked response in relation to the unconditioned (first) response (6, 14, 15, 44). In the current study, paired stimuli delivered with 50-ms interstimuli interval and the anode configured over the anterior neck (*study 1*) produced postactivation depression in all muscles regardless of the cathode configuration (C6, C7, and T1), as previously described (14, 15, 44). Although not statistically significant, suppression of the second responses was also possible when anode configurations other than the anterior neck (Iliac Crests, Shoulders, and Back) were employed with equivalent stimulation intensities (*study 2*; c. f. Fig. 7). These results confirm the predominant reflex origins of the spinally evoked motor responses at multiple cervical spinal segments using various electrode configurations, which suggests that monosynaptic pathways were activated (14, 15, 44). Overall, regardless of the cathode configuration (C6, C7, or T1), postactivation depression in multiple upper-limb muscles may be elicited.

The stimulation intensity (X_D), which yielded the maximal postactivation depression, was not different between the muscles and cathode configurations examined in this study (c.f., X_D in Fig. 5*A*). This suggests that maximal postactivation depression can be elicited simultaneously in multiple upper-limb muscles using the same stimulus intensity (c.f., Fig. 5*A*), as previously suggested (14, 45). Nonetheless, our results also showed that maximal postactivation depression amount (D_{MAX}) was significantly greater in the elbow extensors (TB) compared with elbow flexors (BB) (c.f., D_{MAX} in Fig. 5*A*). Since the amount of reciprocal inhibition between BB and TB to their motor pools was shown to be similar (46), heteronymous projections from other joint muscles (i.e., trans-joint projections) may have contributed to greater inhibition of the TB motor pool. In fact, the strength of projections of Ia fibers from wrist extensor (ECR) and flexor (FCR) muscles onto triceps (TB) motoneurons may have yielded more inhibitory contributions to the recruitment of elbow extensors (47). Although it is possible that that transjoint projections may interfere in the transsynaptic activation of upper limbs during cervical tSCS, further studies are warranted to confirm this.

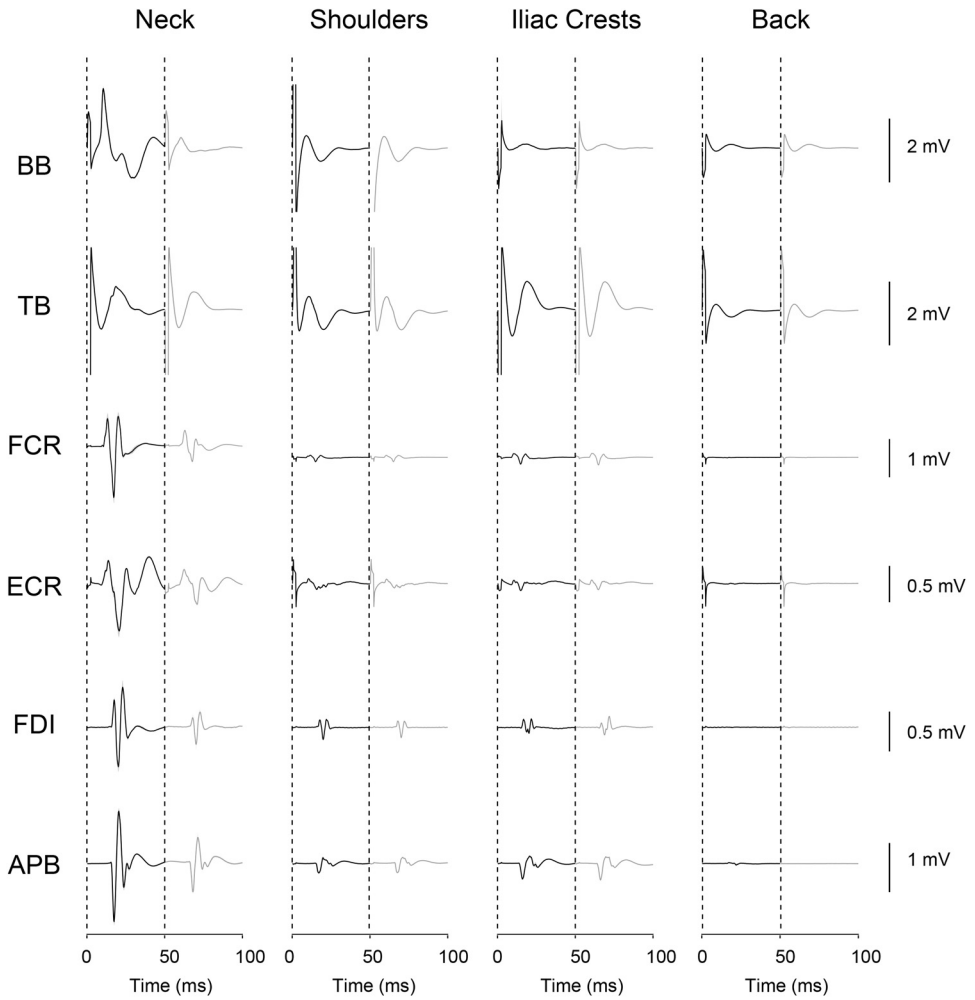

Figure 6. Representative participant averaged responses evoked in the six muscles (BB, TB, FCR, ECR, FDI, and APB) using cervical tSCS with four anode configurations (Neck, Shoulders, Iliac Crests, and Back). Three responses elicited with stimulations delivered as two monophasic pulses (50-ms interstimuli interval) were averaged for each anode configuration with the cathode location and stimulation amplitude chosen specifically for each participant. Representative averaged responses were obtained with the cathode placed over T1 and stimulation intensity at 60 mA. From left to right are the responses elicited with the anode placed the Neck, Shoulders, Iliac Crests, and Back, and from top to bottom are the averaged responses elicited for each muscle. Each trace corresponds to the averaged EMG time series, where the black trace indicates the response elicited by the first stimulus, and the gray trace by the second. The shaded areas in the corresponding colors indicate the standard deviation of the three responses. The dotted lines indicate the instant at which the first and second stimuli were delivered. APB, abductor pollicis brevis; BB, biceps brachii; ECR, extensor carpi radialis; FCR, flexor carpi radialis; FDI, first dorsal interosseous; TB, triceps brachii.

Unlike the observed postactivation depression in the lower-limb muscles (15, 39, 45), our results demonstrated lack of complete abolishment of the second response even at the maximal suppression point (i.e., Fig. 4, which shows postactivation depression at X_D), consistent to Milosevic et al. (14) and Wu et al. (20). It is possible that upper-limb responses during cervical tSCS were not fully suppressed due to antidromic activation of motoneurons, which may reduce the postactivation depression by cancelling synaptic inputs (14). Although unconfirmed, this may also be attributed to shorter poststimulus recovery times of upper-limb responses compared with the lower-limbs, as suggested by Rossi–Durand et al. (48) for explaining the FCR and Soleus H-reflexes responses using paired stimuli. Future investigations should therefore examine different interstimulus intervals on the postactivation depression of the upper-limb muscles using cervical tSCS.

Selectivity and Excitability of Transsynaptic Activation across Different Cervical Vertebral Levels Using tSCS

The selectivity of activation of upper-limb muscles with different cathode locations (C6, C7, and T1) was analyzed through the parameters obtained from the recruitment curves, which estimate excitability attributes of muscle activations using cervical tSCS. Specifically, the stimulus intensity threshold (X_{TH}) and the maximum slope (SL) can be interpreted as excitability factors for the initial recruitment of motoneurons and the increase of the recruitment with increased stimulation current amplitude, respectively. Moreover, the stimulus intensity at 50% of the plateau (X_{50}) can be interpreted as comparative index between X_{TH} and SL (40–42). Our results showed differences between distal hand muscles (FDI and APB) and proximal arm muscles (BB, TB, FCR, and ECR) for X_{TH}, suggesting more excitability to the initial recruitment of motoneurons projecting to proximal arm muscles for all cathodes configurations (c.f., smaller X_{TH} in Fig. 5*B*). Moreover, selectivity to the recruitment of the motoneurons projecting to hand muscles is indicated by the greater values of the SL parameter for T1 cathode configuration compared with C6 and C7 (c.f. SL in Fig. 5*B*). Although not statistically significant, this selectivity is further supported by a decrease of the values of X_{TH} and X_{50} in hand muscles (c.f., differences between proximal and distal muscles for X_{TH} and X_{50} in Fig. 5*B*). Finally, the recruitment curve plateau (PL), which can be interpreted as an index of motor activation, was greater with the cathode electrode configured over T1 compared with C6 in distal hand muscles (c.f., PL in Fig. 5*B*). These findings suggest selectivity of motor pool recruitment of distal muscles with different cathode configurations, which agrees with our hypothesis since distal muscles were preferentially activated with the T1 (caudal) cathode electrode

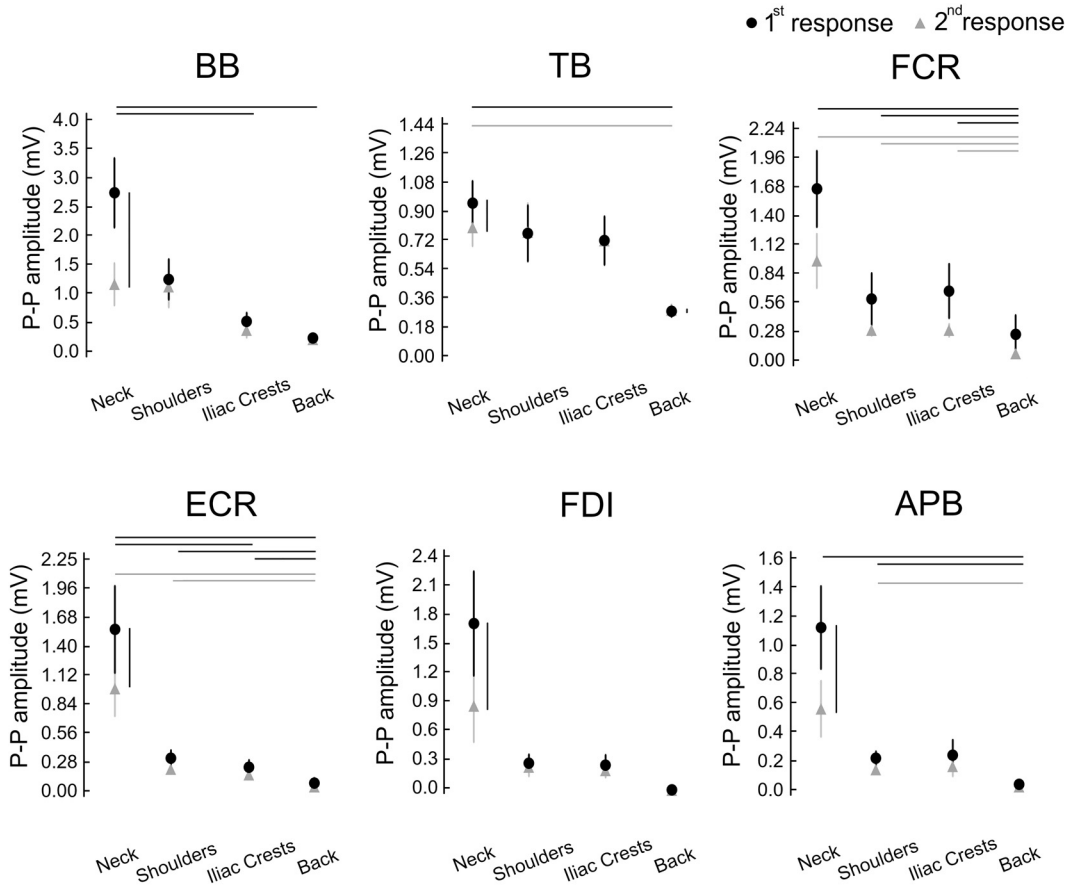

Figure 7. Anodes configurations (*study 2*): the first and the second responses elicited with four anodes configurations (Neck, Shoulders, Iliac Crests, and Back) were compared individually for each muscle. The mean of the first and second responses are indicated with black circles and gray triangles, respectively. Shown are the corresponding standard error vertical bars. The sample size of each data sets is $n = 10$ participants. Significant differences between anode configurations are indicated with black and gray bars for the first and second responses, respectively. Significant differences between the first and second responses are indicated with vertical black bars. APB, abductor pollicis brevis; BB, biceps brachii; ECR, extensor carpi radialis; FCR, flexor carpi radialis; FDI, first dorsal interosseous; TB, triceps brachii.

placement compared with C6 (rostral) vertebral level placement. The three cathode configurations used in this study were chosen based on the more caudal organization of dorsal roots and motor pools projecting distal compared with proximal muscles of human upper-limb (21, 23). Likewise, it is plausible that electrode configurations other than those examined herein (e.g., different sizes and locations) would be selective to the activation of upper-limb motor pools. Nonetheless, despite the larger cathode electrodes (5 × 5 cm) used in the present study compared with previous studies, e.g., 2.5 cm round electrodes used by Gad et al. (4) and Inanici et al. (5), we showed preferential activation of distal hand muscles (FDI and APB) with the T1 cathode configuration. Possibly, configuration of the cathodes more rostrally (e.g., over the C4 vertebra) could preferentially activate proximal upper-limb muscles. Future studies are therefore warranted to test different cathode sizes and more rostral cathode configurations on the responses in upper-limbs using cervical tSCS.

Facilitatory heteronymous projections of the Ia-afferents from distal-to-proximal upper-limb muscles motor pools (47, 49), which are absent from proximal-to-distal muscles in humans (16, 50), may also have contributed to the differences in the activation excitability observed in proximal and distal muscles (X_{TH}). In other words, although the activation of Ia-afferents from distal muscles may contribute to the recruitment of motoneurons of proximal muscles, a mutual relation may not exist from proximal-to-distal muscles in the upper-limbs. In addition, different distributions of motoneuron sizes in hand and arm muscles (51, 52) might have preferentially activated proximal arm muscles through either direct excitation of motor nerves (53), and/or excitation of Ia-monosynaptic pathways (16, 54). Other oligosynaptic pathways connecting group Ib, group II, and cutaneous afferents may also add significant contributions to the motor responses (55). Taken together, different selectivity and excitability factors of recruitment during cervical tSCS may have contributed to preferential activation of distal hand muscles for the T1 cathode configuration, while this was not true for proximal muscles.

The results obtained in the present study inform methodological considerations for placement of the cathode electrode during cervical tSCS to assess spinally evoked motor potentials and/or for rehabilitation protocols using continuous stimulation. For instance, tSCS delivered with the cathode placed over the C6 vertebra [or possibly more rostrally as Gad et al. (4) and Inanici et al. (5)] may be effective to transsynaptically recruit proximal arm muscles, while caudal placement over the T1 vertebrae may be effective for activating distal

Table 3. *Statistical analyses results showing within subject two-way ANOVA interactions and main effect results for postactivation depression (first and second responses) and anode configurations (neck, shoulders, iliac crests, and back) comparisons of the responses evoked in each muscle (BB, TB, FCR, ECR, FDI, and APB) separately*

		Postactivation Depression				Anode	
	Interaction	Neck	Shoulders	Iliac Crest	Back	First	Second
BB	**F (1,9.4) = 16.2 P = 0.003**	**t (9) = 4.2 P = 0.002**	t (9) = 1.6 P = 0.132	t (9) = 1.7 P = 0.121	t (9) = 0.9 P = 0.400	**F (1.4,12.5) = 11.4 P = 0.003**	**F (1.7,15.0) = 4.1 P = 0.044**
TB	**F (3, 27) = 10.4 P < 0.001**	**t (9) = 3.4 P = 0.007**	t (9) = -0.6 P = 0.561	t (9) = 0.3 P = 0.781	**t (9) = -3.2 P = 0.012**	**F (3, 27) = 6.1 P = 0.003**	**F (3, 27) = 4.2 P = 0.014**
FCR	F (1.2,10.8)=3.4 P = 0.087		F (1, 9) = 4.3 P = 0.067			F (3, 27) = 4.5 P < 0.001	
ECR	**F (1,9.2)=9.2 P = 0.013**	**t (9) = 2.8 P = 0.022**	t (9) = 1.7 P = 0.131	t (9) = 1.3 P = 0.219	**t (9) = 1.1 P = 0.296**	**F (1,9.2) = 12.1 P = 0.007**	**F (1,9.2) = 9.3 P = 0.013**
FDI	**F (1.1,10.1)=13.2 P = 0.004**	**t (9) = 3.8 P = 0.004**	t (9) = 1.2 P = 0.260	t (9) = 1.5 P = 0.171	t (9) = 0.5 P = 0.620	**F (1.1,9.5) = 7.9 P = 0.019**	F (1.1,9.8) = 3.7 P = 0.083
APB	**F (1.1,10.3) = 7.5 P = 0.018**	**t (9) = 3.2 P = 0.010**	**t (9) = 2.3 P = 0.048**	t (9) = 1.5 P = 0.160	**t (9) = 2.3 P = 0.048**	**F (1.2,10.6) = 9.7 P = 0.008**	**F (1.1,10.3) = 5.0 P = 0.045**

When interaction was significant, the factors were compared separately with within-subject one-way ANOVA or a t test. Greenhouse–Geisser correction was used when the sphericity assumption was violated. The P values in bold indicate significant differences for a significance level of α = 0.05. APB, abductor pollicis brevis; BB, biceps brachii; ECR, extensor carpi radialis; FCR, flexor carpi radialis; FDI, first dorsal interosseous; TB, triceps brachii.

hand muscles (c.f., Fig. 3). Similarly, stimulation paradigms involving both rostral and caudal cathode electrodes (2, 4, 5) may produce selective activation of cervical spinal networks with tSCS during specific movement tasks. Such preferential activation of arm muscles motor pools may help strength descending commands across spinal lesioned sites during voluntary arm contractions, thus potentially enhancing neuroplasticity effects during rehabilitation (9, 11–13).

Anode Configurations May Optimize Transsynaptic Activation of the Spinally Evoked Responses during Cervical tSCS

The stimulating parameters for comparing anode configurations were chosen to be on the ascending part of the recruitment curve and to yield postactivation depression in the second responses when the anode was placed on the anterior side of the neck. Therefore, responses elicited with other anode configurations (Shoulders, Iliac Crests, and Back) were compared relative to the *neck* configuration. As summarized in Fig. 7, our results indicate that elicited responses were largest when the anode was placed over the anterior neck as well as that postactivation depression was less prevalent when the anodes were not on the anterior neck. Although the proximity between the anode and cathode electrodes and the geometry comprising the cervical body were similar between Shoulders and Neck configuration, our results indicate greater transsynaptic activation with the *neck* configuration compared with the Shoulders. The larger responses yielded with the Neck configuration may not only be due to the proximity between the cathode and anode electrodes, but also a better convergence of the electrical current across the dorsal roots. However, transsynaptic motor activation with other anodes configurations cannot be ruled out and may be elicited using higher stimulation intensities.

Discomfort during tSCS

In our study, the pain experienced during tSCS was not different between the four anode configurations. Participants typically reported discomfort scores between 3 and 5, corresponding to moderate levels of pain (37). Discomforts included skin prickling under the stimulating electrodes and, less commonly, contraction of the neck muscles. It is therefore expected that configuration of the anode electrode over the neck can yield larger spinally evoked responses in the upper-limb muscles (Fig. 7) with similar discomfort levels. Taken together, our results suggest that anterior neck electrode configuration may, at least within the chosen parameters of our study, be more effective in eliciting transsynaptic activation of upper-limb muscles. However, these findings only extent to applications using single and double pulses (i.e., electrophysiological testing), and further testing is required to compare discomfort levels during rehabilitation applications using continuous stimulation.

There were no serious adverse events experienced during the experiments, consistent with previous reports examining cervical tSCS (20, 56). However, it should also be noted that only monophasic double pulses were used with current amplitudes up to 100 mA in the current study.

Limitations

The maximal current intensity was not reached in two participants due to the discomfort experienced, which may have limited the data available for estimating the recruitment curves. Although we used relatively large cathodes (5 × 5 cm) that might have helped alleviate some of the pain felt during stimulation (57, 58), the size of these electrodes could have caused less selectivity for targeting specific upper-limb motor pools (Fig. 5*B*). Despite these limitations, our study showed that it was possible to preferentially activate distal hand muscle with the cathode configured over the T1 level compared with C6 and C7 cathode configurations. Another limitation of the study is the relatively small sample size, despite being comparable to previous studies with able-bodied participants (14, 15, 28, 30, 36, 38). It should also be noted that responses were only recorded unilaterally from the right upper-limb muscles of right-handed participants. It is possible that hand dominance may have influenced the motor

responses (32–34), and thus, our results should be carefully considered and generalized. Finally, despite similar signal-to-noise ratios across muscles in our current study, possible cofounding factors related to comparisons between muscles should further be investigated using non-linear regression models in future studies.

Conclusions

The results obtained in this study showed that transsynaptic activation of motor pools projecting to the upper limb muscles is achievable using all three cathode configurations (C6, C7, and T1). Distal hand muscles (FDI and APB) were preferentially activated with the cathode configured over the T1 vertebra compared with C6 and C7, whereas there was no selectivity for proximal arm muscles (BB, TB, FCR, and ECR). We showed higher stimulation thresholds for activation of distal hand muscles compared with proximal arm muscles. The elicited responses were largest when the anode was placed over the anterior neck, compared with other configurations (Shoulders, Iliac Crests, and Back) with equivalent stimulation intensities. Our results therefore provide methodological considerations for electrode configuration that can help elicit transsynaptic motor activation during cervical tSCS with less current amplitude. The utility of these results concerns the use of tSCS for assessing the state of spinal cord neural circuitries through single and double pulses, whereas further testing is warranted to confirm these findings during continuous stimulation.

GRANTS

This project was funded by the Japan Society for the Promotion of Science Grants-in-Aid for Scientific Research—KAKENHI (Grant Nos.: 19K23606 and 20K19412). We acknowledge support of the Global Center for Medical Engineering and Informatics at Osaka University (MEI Grant B). R. M. de Freitas is supported by the Engineering Science for the 21st Century scholarship granted by the Japanese Ministry of Education, Culture, Sports, Science, and Technology (MEXT).

DISCLOSURES

No conflicts of interest, financial or otherwise, are declared by the authors.

AUTHOR CONTRIBUTIONS

R.M.d.F., A.S., K.N., and M.M. conceived and designed research; A.S. and M.M. performed experiments; R.M.d.F. and A.S. analyzed data; R.M.d.F., D.G.S., Y.M., T.N., K.N., and M.M. interpreted results of experiments; R.M.d.F. and A.S. prepared figures; R.M.d.F., A.S., and M.M. drafted manuscript; R.M.d.F., A.S., D.G.S., Y.M., T.N., K.N., and M.M. edited and revised manuscript; R.M.d.F., A.S., D.G.S., Y.M., T.N., K.N., and M.M. approved final version of manuscript.

REFERENCES

1. **Lu DC**, **Edgerton VR**, **Modaber M**, **AuYong N**, **Morikawa E**, **Zdunowski S**, **Sarino ME**, **Sarrafzadeh M**, **Nuwer MR**, **Roy RR**, **Gerasimenko Y.** Engaging cervical spinal cord networks to reenable volitional control of hand function in tetraplegic patients. *Neurorehabil Neural Repair* 30: 951–962, 2016. doi:10.1177/1545968316644344.
2. **Benavides FD**, **Jo HJ**, **Lundell H**, **Edgerton VR**, **Gerasimenko Y**, **Perez MA.** Cortical and subcortical effects of transcutaneous spinal cord stimulation in humans with tetraplegia. *J Neurosci* 40: 2633–2643, 2020. doi:10.1523/JNEUROSCI.2374-19.2020.
3. **Freyvert Y**, **Yong NA**, **Morikawa E**, **Zdunowski S**, **Sarino ME**, **Gerasimenko Y**, **Edgerton VR**, **Lu DC.** Engaging cervical spinal circuitry with non-invasive spinal stimulation and buspirone to restore hand function in chronic motor complete patients. *Sci Rep* 8: 15546, 2018. doi:10.1038/s41598-018-33123-5.
4. **Gad P**, **Lee S**, **Terrafranca N**, **Zhong H**, **Turner A**, **Gerasimenko Y**, **Edgerton VR.** Non-invasive activation of cervical spinal networks after severe paralysis. *J Neurotrauma* 35: 2145–2158, 2018. doi:10.1089/neu.2017.5461.
5. **Inanici F**, **Samejima S**, **Gad P**, **Edgerton VR**, **Hofstetter CP**, **Moritz CT.** Transcutaneous electrical spinal stimulation promotes long-term recovery of upper extremity function in chronic tetraplegia. *IEEE Trns Neural Syst Rehabil Eng* 26: 1272–1278, 2018. doi:10.1109/TNSRE.2018.2834339.
6. **Hofstoetter US**, **Freundl B**, **Binder H**, **Minassian K.** Common neural structures activated by epidural and transcutaneous lumbar spinal cord stimulation: elicitation of posterior root-muscle reflexes. *PLoS One* 13: e0192013, 2018. doi:10.1371/journal.pone.0192013.
7. **Capogrosso M**, **Wenger N**, **Raspopovic S**, **Musienko P**, **Beauparlant J**, **Bassi Luciani L**, **Courtine G**, **Micera S.** A computational model for epidural electrical stimulation of spinal sensorimotor circuits. *J Neurosci* 33: 19326–19340, 2013. doi:10.1523/JNEUROSCI.1688-13.2013.
8. **Danner SM**, **Hofstoetter US**, **Ladenbauer J**, **Rattay F**, **Minassian K.** Can the human lumbar posterior columns be stimulated by transcutaneous spinal cord stimulation? A modeling study. *Artif Organs* 35: 257–262, 2011. [Erratum in Artif Organs. 2011 May;35(5):556]. doi:10.1111/j.1525-1594.2011.01213.x.
9. **Formento E**, **Minassian K**, **Wagner F**, **Mignardot JB**, **Le Goff-Mignardot CG**, **Rowald A**, **Bloch J**, **Micera S**, **Capogrosso M**, **Courtine G.** Electrical spinal cord stimulation must preserve proprioception to enable locomotion in humans with spinal cord injury. *Nat Neurosci* 21: 1728–1741, 2018. doi:10.1038/s41593-018-0262-6.
10. **Wagner FB**, **Mignardot J-B**, **Le Goff-Mignardot CG**, **Demesmaeker R**, **Komi S**, **Capogrosso M**, et al**.** Targeted neurotechnology restores walking in humans with spinal cord injury. *Nature* 563: 65–71, 2018. doi:10.1038/s41586-018-0649-2.
11. **Courtine G**, **Sofroniew MV.** Spinal cord repair: advances in biology and technology. *Nat Med* 25: 898–908, 2019. doi:10.1038/s41591-019-0475-6.
12. **Murray LM**, **Knikou M.** Transspinal stimulation increases motoneuron output of multiple segments in human spinal cord injury. *PLoS One* 14: e0213696, 2019. doi:10.1371/journal.pone.0213696.
13. **Park S-W**, **Wolf SL**, **Blanton S**, **Winstein C**, **Nichols-Larsen DS.** The EXCITE Trial: predicting a clinically meaningful motor activity log outcome. *Neurorehabil Neural Repair* 22: 486–493, 2008. doi:10.1177/1545968308316906.
14. **Milosevic M**, **Masugi Y**, **Sasaki A**, **Sayenko DG**, **Nakazawa K.** On the reflex mechanisms of cervical transcutaneous spinal cord stimulation in human subjects. *J Neurophysiol* 121: 1672–1679, 2019. doi:10.1152/jn.00802.2018.
15. **Minassian K**, **Persy I**, **Rattay F**, **Dimitrijevic MR**, **Hofer C**, **Kern H.** Posterior root–muscle reflexes elicited by transcutaneous stimulation of the human lumbosacral cord. *Muscle Nerve* 35: 327–336, 2007. doi:10.1002/mus.20700.
16. **Pierrot-Deseilligny E**, **Burke , D.** *The Circuitry of the Human Spinal Cord*. Cambridge, UK: Cambridge University Press, 2005.
17. **Greiner N**, **Barra B**, **Schiavone G**, **Lorach H**, **James N**, **Conti S**, **Kaeser M**, **Fallegger F**, **Borgognon S**, **Lacour S**, **Bloch J**, **Courtine G**, **Capogrosso M.** Recruitment of upper-limb motoneurons with epidural electrical stimulation of the cervical spinal cord. *Nat Commun* 12: 435, 2021. doi:10.1038/s41467-020-20703-1.
18. **Zheng Y**, **Hu X.** Elicited upper limb motions through transcutaneous cervical spinal cord stimulation. *J Neural Eng* 17: 036001, 2020. doi:10.1088/1741-2552/ab8f6f.
19. **Zheng Y**, **Hu X.** Muscle activation pattern elicited through transcutaneous stimulation near the cervical spinal cord. *J Neural Eng* 17: 016064, 2020. doi:10.1088/1741-2552/ab5e09.
20. **Wu YK**, **Levine JM**, **Wecht JR**, **Maher MT**, **LiMonta JM**, **Saeed S**, **Santiago TM**, **Bailey E**, **Kastuar S**, **Guber KS**, **Yung L**, **Weir JP**, **Carmel JB**, **Harel NY.** Posteroanterior cervical transcutaneous

spinal stimulation targets ventral and dorsal nerve roots. *Clin Neurophysiol* 131: 451–460, 2020. doi:10.1016/j.clinph.2019.11.056.
21. **Cadotte DW**, **Cadotte A**, **Cohen-Adad J**, **Fleet D**, **Livne M**, **Wilson JR**, **Mikulis D**, **Nugaeva N**, **Fehlings MG.** Characterizing the location of spinal and vertebral levels in the human cervical spinal cord. *AJNR Am J Neuroradiol* 36: 803–810, 2015. doi:10.3174/ajnr.A4192.
22. **Cramer GD**, **Darby , SA.** Clinical anatomy of the spine, *Spinal Cord, and ANS*. 3rd Ed. St. Louis, Missouri: Elsevier Health Sciences, 2013.
23. **Kendall FP**, **Kendall EM**, **Provance PG**, **Rodgers MM**, **Romani , WA.** *Muscles: Testing and Function with Posture and Pain*. 5th ed. Philadelphia, PA: Lippincott, Williams, & Wilkins, 2005.
24. **Islam MA**, **Zaaya M**, **Comiskey E**, **Demetrio J**, **O'Keefe A**, **Palazzo N**, **Pulverenti TS**, **Knikou M.** Modulation of soleus H-reflex excitability following cervical transspinal conditioning stimulation in humans. *Neurosci Lett* 732: 135052, 2020. doi:10.1016/j.neulet.2020.135052.
25. **Murray LM**, **Knikou M.** Remodeling brain activity by repetitive cervicothoracic transspinal stimulation after human spinal cord injury. *Front Neurol* 8, 2017. doi:10.3389/fneur.2017.00050.
26. **Massey SJ.** ***Al'joboori YD***, ***Vanhoestenberghe A***, ***Duffell LD***. *The Effects of Neuromodulation on Central Excitability of the Upper Limb in* Healthy, Able-bodied Adults. In: International Functional Electrical Stimulation Society Proceedings. 2018.
27. **Villar Ortega E**, **Ansó J**, **Bütler KA**, **Marchal-Crespo , L.** High-frequency transcutaneous cervical electrical stimulation: A pilot study. In: *13th Vienna International Workshop on Functional Electrical Stimulation*. 2019.
28. **Krenn M**, **Toth A**, **Danner SM**, **Hofstoetter US**, **Minassian K**, **Mayr W.** Selectivity of transcutaneous stimulation of lumbar posterior roots at different spinal levels in humans. *Biomed Eng/Biomed Tech* 58, 2013. doi:10.1515/bmt-2013-4010.
29. **Roy FD**, **Gibson G**, **Stein RB.** Effect of percutaneous stimulation at different spinal levels on the activation of sensory and motor roots. *Exp Brain Res* 223: 281–289, 2012. doi:10.1007/s00221-012-3258-6.
30. **Sayenko DG**, **Atkinson DA**, **Dy CJ**, **Gurley KM**, **Smith VL**, **Angeli C**, **Harkema SJ**, **Edgerton VR**, **Gerasimenko YP.** Spinal segment-specific transcutaneous stimulation differentially shapes activation pattern among motor pools in humans. *J Appl Physiol (1985)* 118: 1364–1374, 2015. doi:10.1152/japplphysiol.01128.2014.
31. **Oldfield RC.** The assessment and analysis of handedness: The Edinburgh inventory. *Neuropsychologia* 9: 97–113, 1971. doi:10.1016/0028-3932(71)90067-4.
32. **Gordon NM**, **Rudroff T**, **Enoka JA**, **Enoka RM.** Handedness but not dominance influences variability in endurance time for sustained, submaximal contractions. *J Neurophysiol* 108: 1501–1510, 2012. doi:10.1152/jn.01144.2011.
33. **Pereira R**, **Freire IV**, **Cavalcanti CVG**, **Luz CPN**, **Neto OP.** Hand dominance during constant force isometric contractions: evidence of different cortical drive commands. *Eur J Appl Physiol* 112: 2999–3006, 2012. doi:10.1007/s00421-011-2278-4.
34. **Sathiamoorthy A**, **Sathiamoorthy SS.** Limb dominance and motor conduction velocity of median and ulnar nerves. *Indian J Physiol Pharmacol* 34: 51–53, 1990.
35. **Kitano K**, **Koceja DM.** Spinal reflex in human lower leg muscles evoked by transcutaneous spinal cord stimulation. *J Neurosci Methods* 180: 111–115, 2009. doi:10.1016/j.jneumeth.2009.03.006.
36. **Danner SM**, **Krenn M**, **Hofstoetter US**, **Toth A**, **Mayr W**, **Minassian K.** Body position influences which neural structures are recruited by lumbar transcutaneous spinal cord stimulation. *PLoS One* 11: e0147479, 2016. doi:10.1371/journal.pone.0147479.
37. **Hawker GA**, **Mian S**, **Kendzerska T**, **French , M.** Measures of adult pain: Visual Analog Scale for Pain (VAS Pain), Numeric Rating Scale for Pain (NRS Pain), *McGill Pain Questionnaire (MPQ)*, Short-Form McGill Pain Questionnaire (SF-MPQ), Chronic Pain Grade Scale (CPGS), Short Form-36 Bodily Pain Scale (SF. *Arthritis Care Res (Hoboken)* 63: S240–S252, 2011. doi: 10.1002/acr.20543..
38. **Courtine G**, **Harkema SJ**, **Dy CJ**, **Gerasimenko YP**, **Dyhre-Poulsen P.** Modulation of multisegmental monosynaptic responses in a variety of leg muscles during walking and running in humans. *J Physiol* 582: 1125–1139, 2007. doi:10.1113/jphysiol.2007.128447.
39. **Sayenko DG**, **Atkinson DA**, **Floyd TC**, **Gorodnichev RM**, **Moshonkina TR**, **Harkema SJ**, **Edgerton VR**, **Gerasimenko YP.** Effects of paired transcutaneous electrical stimulation delivered at single and dual sites over lumbosacral spinal cord. *Neurosci Lett* 609: 229–234, 2015. doi:10.1016/j.neulet.2015.10.005.
40. **Devanne H**, **Lavoie BA**, **Capaday C.** Input-output properties and gain changes in the human corticospinal pathway. *Exp Brain Res* 114: 329–338, 1997. doi:10.1007/PL00005641.
41. **Smith AC**, **Rymer WZ**, **Knikou M.** Locomotor training modifies soleus monosynaptic motoneuron responses in human spinal cord injury. *Exp Brain Res* 233: 89–103, 2015. doi:10.1007/s00221-014-4094-7.
42. **Capaday C.** Neurophysiological methods for studies of the motor system in freely moving human subjects. *J Neurosci Methods* 74: 201–218, 1997. doi:10.1016/s0165-0270(97)02250-4.
43. **Sekiguchi H**, **Nakazawa K**, **Suzuki S.** Differences in recruitment properties of the corticospinal pathway between lengthening and shortening contractions in human soleus muscle. *Brain Res* 977: 169–179, 2003. doi:10.1016/s0006-8993(03)02621-0.
44. **Hofstoetter US**, **McKay WB**, **Tansey KE**, **Mayr W**, **Kern H**, **Minassian K.** Modification of spasticity by transcutaneous spinal cord stimulation in individuals with incomplete spinal cord injury. *J Spinal Cord Med* 37: 202–211, 2014. doi:10.1179/2045772313Y.0000000149.
45. **Milosevic M**, **Masugi Y**, **Obata H**, **Sasaki A**, **Popovic MR**, **Nakazawa K.** Short-term inhibition of spinal reflexes in multiple lower limb muscles after neuromuscular electrical stimulation of ankle plantar flexors. *Exp Brain Res* 237: 467–476, 2019. doi:10.1007/s00221-018-5437-6.
46. **Katz R**, **Penicaud A**, **Rossi A.** Reciprocal Ia inhibition between elbow flexors and extensors in the human. *J Physiol* 437: 269–286, 1991. doi:10.1113/jphysiol.1991.sp018595.
47. **Cavallari P**, **Katz R.** Pattern of projections of group I afferents from forearm muscles to motoneurones supplying biceps and triceps muscles in man. *Exp Brain Res* 78, 1989. doi:10.1007/BF00230235.
48. **Rossi-Durand C**, **Jones KE**, **Adams S**, **Bawa P.** Comparison of the depression of H-reflexes following previous activation in upper and lower limb muscles in human subjects. *Exp Brain Res* 126: 117–127, 1999. doi:10.1007/s002210050721.
49. **Marchand -Pauvert V**, **Nicolas G**, **Pierrot -Deseilligny E.** Monosynaptic Ia projections from intrinsic hand muscles to forearm motoneurones in humans. *J Physiol* 525: 241–252, 2000. doi:10.1111/j.1469-7793.2000.t01-1-00241.x.
50. **Cavallari P**, **Katz R**, **Penicaud A.** Pattern of projections of group I afferents from elbow muscles to motoneurones supplying wrist muscles in man. *Exp Brain Res* 91, 1992. doi:10.1007/BF00231664.
51. **Enoka RM.** *Neuromechanics of Human Movement*. 4th Ed. Champaign, IL: Human Kinetics, 2015.
52. **Enoka RM**, **Fuglevand AJ.** Motor unit physiology: some unresolved issues. *Muscle Nerve* 24: 4–17, 2001. doi:10.1002/1097-4598(200101)24:1<4::AID-MUS13>3.0.CO;2-F.
53. **Rattay F.** The basic mechanism for the electrical stimulation of the nervous system. *Neuroscience* 89: 335–346, 1999. doi:10.1016/s0306-4522(98)00330-3.
54. **Buller NP**, **Garnett R**, **Stephens JA.** The reflex responses of single motor units in human hand muscles following muscle afferent stimulation. *J Physiol* 303: 337–349, 1980. doi:10.1113/jphysiol.1980.sp013289.
55. **Gerasimenko Y**, **Gorodnichev R**, **Moshonkina T**, **Sayenko D**, **Gad P**, **Reggie Edgerton V.** Transcutaneous electrical spinal-cord stimulation in humans. *Ann Phys Rehabil Med* 58: 225–231, 2015. doi:10.1016/j.rehab.2015.05.003.
56. **Sabbahi MA**, **Sengul YS.** Cervical multisegmental motor responses in healthy subjects. *Spinal Cord* 50: 432–439, 2012. doi:10.1038/sc.2011.166.
57. **Roy FD**, **Bosgra D**, **Stein RB.** Interaction of transcutaneous spinal stimulation and transcranial magnetic stimulation in human leg muscles. *Exp Brain Res* 232: 1717–1728, 2014. doi:10.1007/s00221-014-3864-6.
58. **Verhoeven K**, **van Dijk JG.** Decreasing pain in electrical nerve stimulation. *Clin Neurophysiol* 117: 972–978, 2006. doi:10.1016/j.clinph.2006.01.006.